ACS OMEGA

Article

Cite This: ACS Omega 2018, 3, 14188−14200

http://pubs.acs.org/journal/acsodf

Modified Thermal, Dielectric, and Electrical Conductivity of PVDF-HFP/$LiClO_4$ Polymer Electrolyte Films by 8 MeV Electron Beam Irradiation

Yesappa Laxmayyaguddi, Niranjana Mydur, Ashokkumar Shankar Pawar, Vijeth Hebri, M. Vandana, Ganesh Sanjeev, and Devendrappa Hundekal*

Department of Physics, Mangalore University, Mangalagangothri, Mangaluru 574199, India

ABSTRACT: The polymer electrolyte films (poly-((vinylidene fluoride)-*co*-hexafluoropropylene)/$LiClO_4$@ 90:10 w/w, PHL10) were prepared by solution-casting technique and the effect of various dosages of electron beam (EB) irradiation on structure, morphology, thermal, dielectric, and conductivity properties at various dosages. The atomic force microscope topography image shows substantial change in surface morphology due to irradiation and the modification of chemical bonds through chain scission process with increased EB dose was confirmed by Fourier transform infrared spectroscopy studies. NMR studies confirm the change in structural properties due to irradiation. The X-ray diffractometer confirms the decreased crystallinity from 50.10 for unirradiated film to 40.96 at 120 kGy doses; hence, increase in amorphousity due to a decrease in melting temperature from 460 to 418 °C leads to the degradation of the polymer, and the differential scanning calorimetry study reveals the decreased crystallinity with increased irradiation dose. The dielectric and modulus parameters are observed to decrease with increasing frequency as well as temperature. The conductivity increases with frequency and EB dose due to the increased segmental motion of charged ions by chain scission/cross-linking process. The high conductivity of 1.81×10^{-3} S/cm with the corresponding relaxation time of 1.697×10^{-6} at 120 kGy dose was observed. The conduction mechanism reveals an Ohmic behavior and the $I-V$ plot exhibits a gradual increase in current with applied voltage as well as irradiation dose. The electrochemical performance of the irradiated polymer electrolyte was improved significantly and hence the polymer electrolytes can be used in solid-state batteries and storage applications after altering the properties by the influence of irradiation.

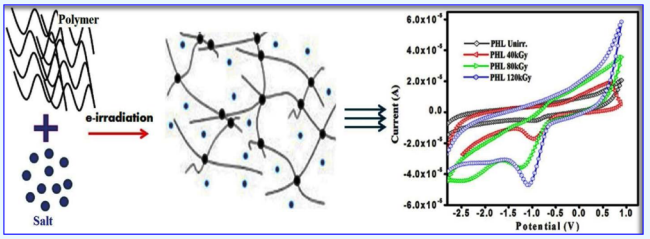

1. INTRODUCTION

Polymers have been used in many potential applications due to their excellent physical properties and in various potential applications such as safety systems of nuclear power plants after exposure to various radiation energies, medical usage, packing, optoelectronics,[1] and others. However, modification of physical properties by irradiation has become an attractive area.[2] Many investigations have revealed that the interaction of radiations with polymers leads to rupture of the chemical bonds of the polymer chain, resulting in the formation of polymer fragments and free radicals.[2,3] These changes in polymer chain caused by the occurrence of chain scission/cross-linking as a result of rearrangement in the molecular-level microstructure or change in chemistry.[4,5] The effect of radiation on the polymer depends on many factors, like energy, type of radiation and dosimetry conditions, and chemical and physical properties of the polymer. From literature, it has seen that various irradiation techniques have been used to modify the physical properties of the polymer.[6,7] There are various radiation energies such as electron beam (EB), γ, ions, X-ray, ultraviolet; among these, the electron beam (EB) irradiation is a rapidly developing technique owing to its simple and pollution-free use to improve the physiochemical properties of the polymers.[8] It can change the structure and thermal properties of copolymers and also break the crystal into micropolar regions that interact only through electrostatic coupling.[9] The degree of crystallinity of the polymer electrolytes have been reported to decrease in most of the semicrystalline polymers at high dose irradiation.[10] The copolymers after exposure to high energies can exhibit high electromechanical performance, and such materials are used in sensor and transducer applications.[11] It is also important to understand the charge transport mechanism in the polymers by studying the electrical conductivity and dielectric relaxation upon EB irradiation.[6,12] Few studies have reported changes in thermal property, structural arrangement, surface morphology, and electrical conductivity upon EB irradiation on copolymers like polypropylene, poly(vinyl chloride), etc.[13,14] In the present case, poly((vinylidene fluoride)-*co*-hexafluoropropylene) (PVDF-HFP) is one of the copolymer considered as a suitable host due to various interesting properties like high dielectric constant (ε = 8.4) that support dissociation of salts like Na^+ and Li^+, low crystallinity, which can improve conductivity. Excellent

Received: May 23, 2018
Accepted: August 21, 2018
Published: October 26, 2018

DOI: 10.1021/acsomega.8b01097
ACS Omega 2018, 3, 14188−14200

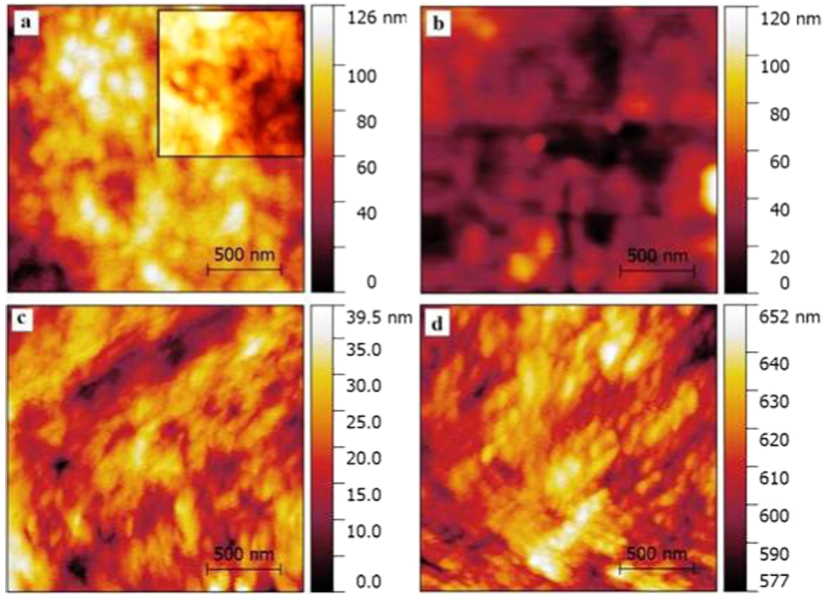

Figure 1. Atomic force microscopic images of (a) PHL unirradiated (inset, PVDF-HFP) and irradiated with (b) 40 kGy, (c) 80 kGy, and (d) 120 kGy dosage.

chemical stability due to crystalline phase vinylidene supported by hexafluoropropylene (HFP) in amorphous phase and possibilities of new applications like optoelectronic devices, sensor, supercapacitor, medical radiation therapy, and food processing[13,15] are the reasons irradiation of copolymer has been receiving more attention. The polymer electrolytes based on lithium salts have been preferably studied because Li^+ cations are the smallest and can easily move in a polymer matrix through transient coordinate bonds and improves the ion-transport process. Hence, the present study investigated the effects of EB irradiation on thermal, dielectric, and conductivity of PVDF-HFP/$LiClO_4$ polymer electrolytes and reported the modifications.

2. CHARACTERIZATION TECHNIQUES

The unirradiated and irradiated polymer electrolyte films were characterized by using various techniques; the atomic force microscopy (AFM) in noncontact mode is used to study the surface topology. The Fourier transform infrared spectroscopy (FT-IR) measurement was done with the help of Bruker Alpha Eco ATR FT-IR spectroscopy between 500 and 3000 cm^{-1} ranges and Bruker ascend 400 MHz NMR spectrometer is used to record the ^{13}C NMR spectra at room temperature using dimethyl sulfoxide as solvent. The Rigaku Miniflex 500 tabletop powder X-ray diffraction (XRD) is used to study the structural properties of materials. Thermogravimetric analysis (TGA), differential thermal analysis (DTA), and differential scanning calorimetry (DSC) are studied using TA instruments Q-600 heating from 30 to 700 °C at the heating rate of 10 °C/min under nitrogen flow rate of approximately 20 mL/min. The dielectric measurement was done by Wayne Kerr Precision Impedance Analyser 6500B in the frequency range 40 Hz to 1 MHz and at different temperatures. Cyclic voltammeter analysis was done by using the CHI-660E electrochemical workstation at room temperature.

3. RESULTS AND DISCUSSION

3.1. Atomic Force Microscopic Study of Unirradiated and Irradiated Film. The surface roughness factor of the PHL10 polymer electrolyte films before and after irradiation was studied by AFM images as shown in Figure 1a–d. The change in root mean square (RMS) roughness values has observed after exposure to EB irradiation.

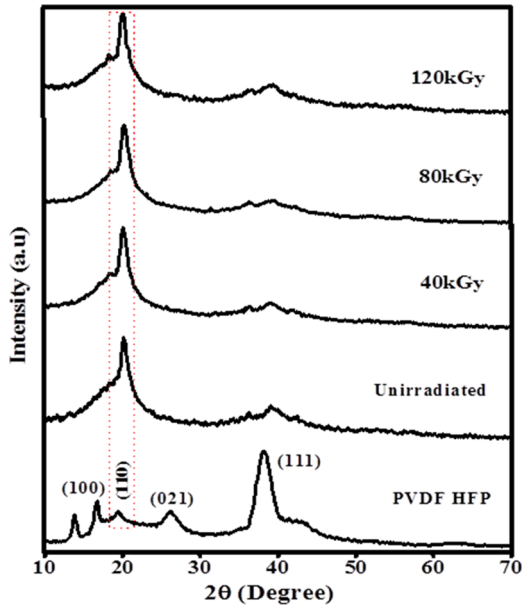

Figure 2. Powder X-ray diffraction patterns of PHL electrolyte before and after EB irradiation.

The host polymer PVDF-HFP exhibits the RMS value of 120.9 nm, which decreases to 116.5 nm for unirradiated PHL10 film, confirming the formation of complexation. The modified surface of polymer electrolytes due to irradiation effect is shown in Figure 1b–d, note the RMS values increased to 117.6, 121.8, and 123.4 nm for 40, 80, and 120 kGy doses, respectively.[16,17] The significant change in surface morphology with increased EB dose confirms that the polymer degradation increases the amorphous phase in polymer electrolytes after irradiation.[18,19]

DOI: 10.1021/acsomega.8b01097
ACS Omega 2018, 3, 14188–14200

Table 1. Estimated XRD Data of d (Å), Full Width at Half-Maxima (β), Crystallite Separation R (Å), Strain (ε), Crystallite Size, D (Å), and Percentage of Crystallinity (χ)

sample	2θ	d (Å)	β	R (Å)	ε	D (Å)	% χ
PVDF-HFP	19.40	4.45	7.3773	5.68	1.81	0.20	53.46
	38.3	2.34	2.3923	2.93	0.56	0.64	46.80
PHL unirr.	20.10	4.41	2.0979	5.51	0.51	0.70	50.10
PHL 40 kGy	20.19	4.39	1.9954	5.49	0.49	0.73	48.13
PHL 80 kGy	20.20	4.39	2.0915	5.48	0.51	0.72	46.61
PHL 120 kGy	20.09	4.41	2.2941	5.52	0.56	0.64	40.96
	38.90	2.31	4.8962	2.89	1.15	0.31	38.74

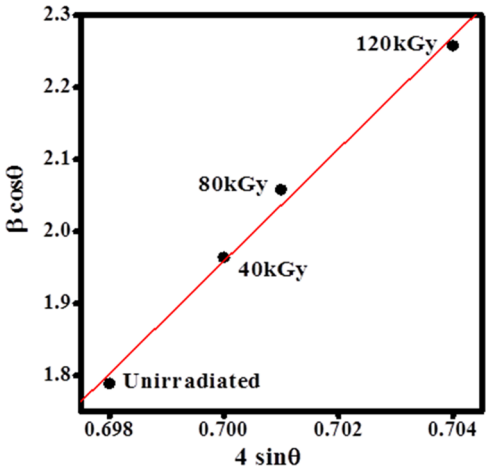

Figure 3. Williamson–Hall plots for PHL electrolyte before and after EB irradiation.

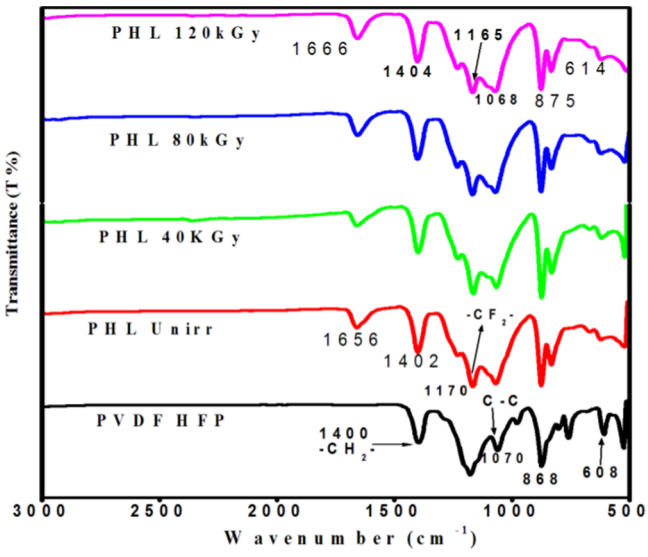

Figure 4. FT-IR spectra of PHL10 polymer electrolyte before and after EB irradiation at different dosages.

3.2. X-ray Diffraction Study of Unirradiated and Irradiated Film. X-ray diffractograms of unirradiated and irradiated PHL10 polymer films are shown in Figure 2. The XRD peaks observed at 2θ = 16.79, 19.49, and 26.19° illustrate the partial semicrystalline nature of pure PVDF-HFP.[15,20,21] When PHL10 electrolyte film is exposed to EB energy, it observed that the disappearance of peak at 2θ = 16.79 and 26.19 with corresponding planes (100), (021) indicates the amorphous state of the polymer[21] and at 2θ = 38.30° with plane (111) intensity significantly decreased and becomes broader for 120 kGy dose. The broadening and increase in intensity of the crystalline peak of the unirradiated film at 2θ = 19.90° plane (110) upon irradiation dose confirm the decrease in crystallite size. The prominent peak observed at $2\theta(111)$ = 38.30° for PVDF-HFP electrolyte was found to decrease significantly with irradiation and shifted to $2\theta(111)$ = 38.90° for 120 kGy dose, confirming the decrease in crystallinity by chain scissoning process; the results were in agreement with earlier report.[10] The observed results noticed change in the crystalline phase of the polymer electrolyte after EB irradiation due to formation of defect states, resulting in destruction of the polymer chain by high radiation energy.

Using Debye–Scherrer equation, for every θ (sharp peaks) values, the average crystallite separation (R), strain (ε), crystallite size (D), and percentage of crystallinity (χ) were calculated using the following equations

$$R = \frac{5\lambda}{8 \sin \theta} \quad (1)$$

$$\varepsilon = \frac{\beta \cos \theta}{4} \quad (2)$$

$$D = \frac{k\lambda}{\beta \cos \theta} \quad (3)$$

$$X_c = \frac{A_c}{A_c + A_a} \quad (4)$$

where k is the shape factor, whose value is assumed to be 0.9, λ is the wavelength of the X-ray with value of 0.154 Å, and A_c and A_a are the areas under crystalline and amorphous peaks, respectively, and the calculated parameters are presented in Table 1. The average crystallite size and strain values were calculated for the unirradiated and irradiated polymer electrolytes at 40, 80, and 120 kGy using the Williamson–Hall method as shown in Figure 3.

Figure 2 clearly shows that the crystalline peak of the unirradiated film at 2θ = 19.49° broadens and the intensity increases with increase in the EB dose and the full-width at half maximum also increases, indicating a decrease in the crystallite size. The results show that a decrease in the degree of crystallinity confirms an increase in the amorphous region and is attributed to the degradation of the polymer chains.[22] The obtained results are in good agreement with the AFM and FT-IR results.

3.3. FT-IR Spectroscopy Study of Unirradiated and Irradiated Film. A comparison of the peak intensity and shift of the FT-IR spectra of unirradiated film and EB-irradiated PHL10 polymer electrolyte at different EB doses is presented in Figure 4. The spectra change with increase in EB dose. The

DOI: 10.1021/acsomega.8b01097
ACS Omega 2018, 3, 14188–14200

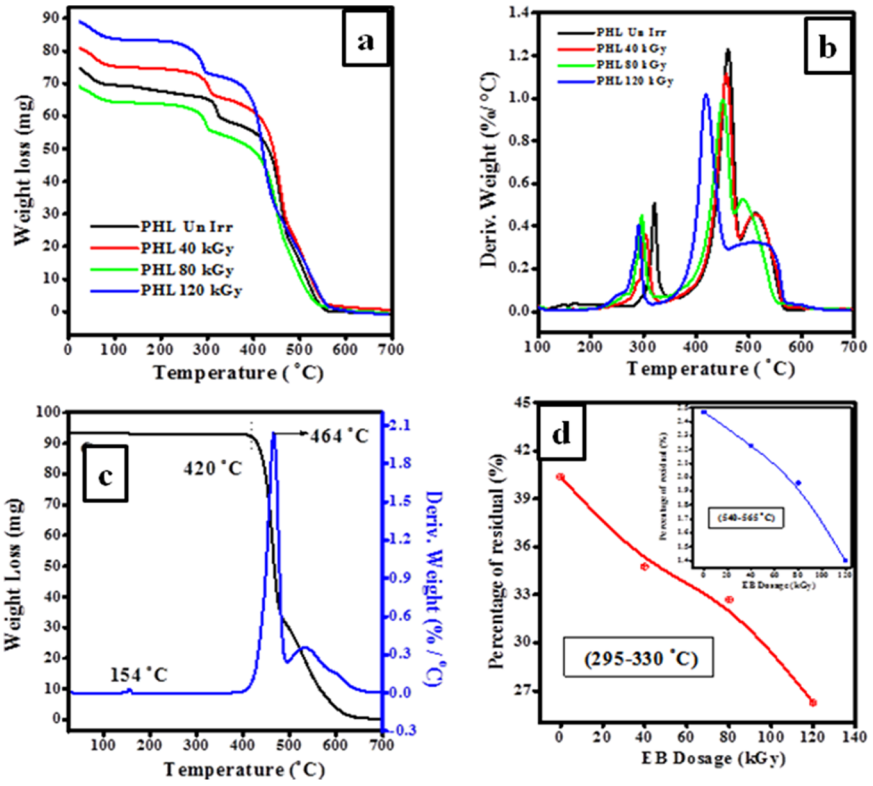

Figure 5. Curves of (a) TGA and (b) DTA of unirradiated and irradiated polymer electrolyte films. (c) TG/DT curves for pure PVDF-HFP. (d) Percentage of residual against EB irradiation dosage in the temperature range 295−330 and 540−565 °C.

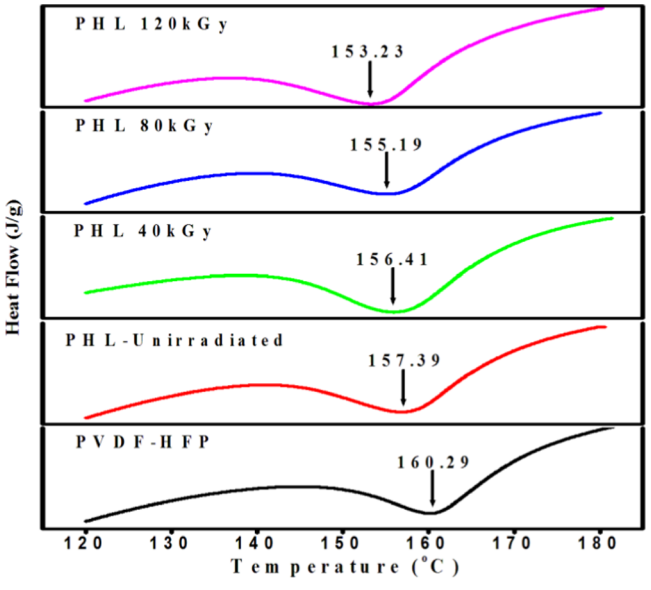

Figure 6. DSC curves of PVDF-HFP/$LiClO_4$ (90:10) polymer electrolytes before and after EB irradiation at different dosages.

change and shift in the vibrational bands of PVDF-HFP observed at 1070, 868, and 608 to 1075, 870, and 610 cm^{-1} with reducing peak intensity after doping with $LiClO_4$ salt confirmed the complexity between salt and polymer matrix (unirradiated). The shift in the band of unirradiated electrolyte from 1656 to 1666 cm^{-1} for 120 kGy was assigned to the C═O bond stretching, confirming the degradation of polymer electrolyte after irradiation.[23] The shift in the band of vinylidene group of host polymer from 1402 to 1404 cm^{-1}

Table 2. Estimated DSC Data of Melting Temperature (°C), Melting Enthalpy (ΔH_m), and Percentage of Crystallinity (χ_c)

samples	T_m (°C)	ΔH_m (J/g)	X_c (%)
PVDF-HFP	160.29	52.46	50.10
PHL unirr.	157.39	52.22	49.84
PHL 40 kGy	156.41	48.00	45.84
PHL 80 kGy	155.19	46.43	44.34
PHL 120 kGy	153.23	33.56	32.05

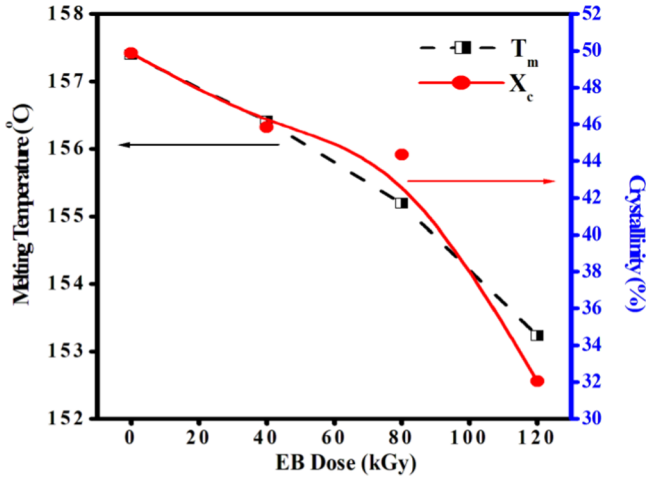

Figure 7. Variation in melting temperature and percentage of crystallinity of PVDF-HFP/$LiClO_4$ polymer electrolytes against EB irradiation dose.

DOI: 10.1021/acsomega.8b01097
ACS Omega 2018, 3, 14188−14200

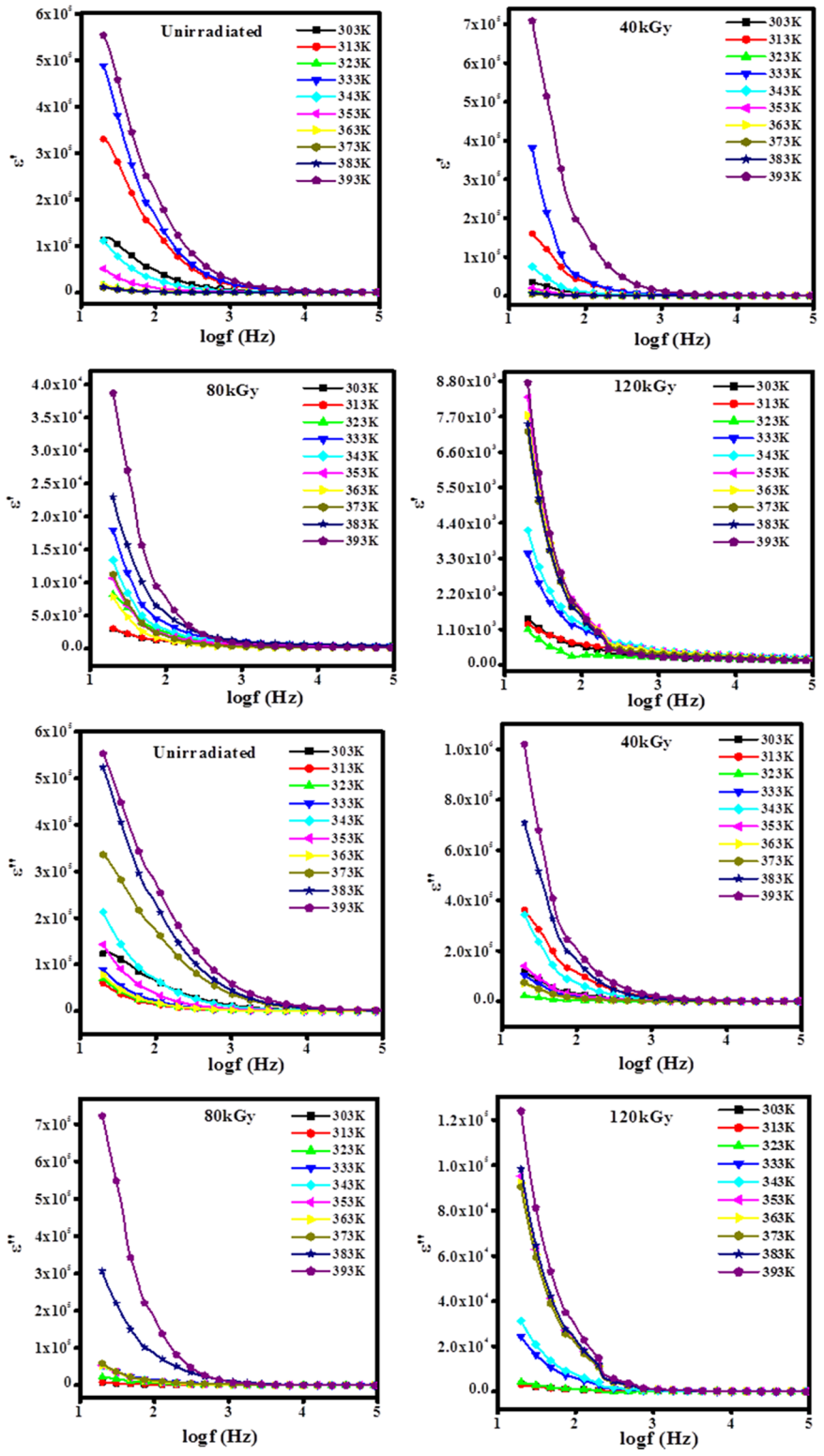

Figure 8. Variation in dielectric constant (ε') and dielectric loss (ε'') with frequency at different temperatures for unirradiated and EB-irradiated PHL10 electrolyte films.

at 120 kGy is attributed to the deformation of the CH_2 band due to C−H bond scissioring upon increased irradiation dosage. The band at 1170 assigned to the CF_2 bond without irradiation was shifted to 1168 after irradiation with 120 kGy EB dose with significant decrease in peak intensity, indicating increased amorphousity in the irradiated polymer electrolyte due to the formation of defects by high radiation energy, in turn, confirming the predominant chain scission and cross-linking processes in polymer electrolyte due to EB irradiation.[24]

The observed results confirm that the EB irradiation can modify the chemical bonds through oxidative chain scission process and increase the amorphousity in the polymer electrolyte; this was clearly reported in our previous

DOI: 10.1021/acsomega.8b01097
ACS Omega 2018, 3, 14188−14200

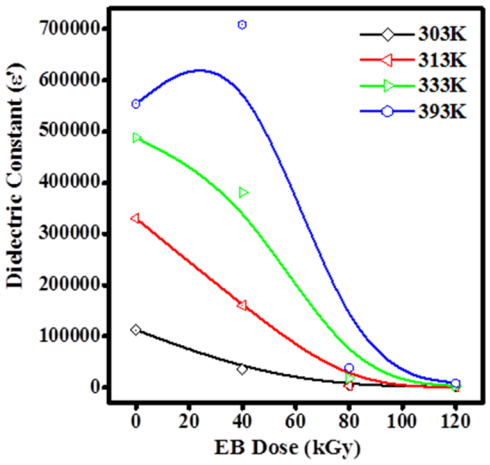

Figure 9. Plot of the variation in the dielectric constant of PHL10 films with dosage.

publication.[25] It can be illustrated that the decrease in peak intensity (transmittance increases) with increase in the dose to 120 kGy results from the cross-linking and the decrease in transmittance with increase in the irradiation dose is attributed to the predomination of chain scission over cross-linking with increasing EB dose.[26] The observed results confirm the alteration in structural properties after EB irradiation.

3.4. Thermal Analysis of Unirradiated and Irradiated Film. TGA/DTA is used to study the thermal stability and degradation of PHL10 polymer electrolyte films before and after irradiation, as shown in Figure 5a,b. The thermogram reveals that a single weight loss in the temperature range of 420−480 °C for pure PVDF-HFP is attributed to the degradation of the polymer backbone and the DTA curve presents an endothermic peak at 154 °C, as shown in Figure 5c, which is associated with the melting temperature of the crystalline phase of the PVDF-HFP.[27] Three major weight loss regions are observed in the TG curves; the first stage, at around 105 °C, is due to the loss of water content, suggesting first degradation step of carbon−hydrogen bond scission and leads to the formation of hydrogen fluoride bonds. The second stage in the range 110−320 °C is the loss of dopant from the polymer matrix; therefore, complex degradation process results in decrease in degradation temperatures to 321, 302, 297, and 290 °C in DTA for unirradiation, 40, 80, and 120 kGy doses, respectively. It is clear from the observed results that the thermal stability of the polymer electrolyte films increased with increase in dose.[28]

The third major loss in 330−565 °C (residual decomposition) was attributed to the destruction of polymeric chain backbone by decrease in degradation temperatures to 460, 456, 450, and 418 °C in DTA corresponding to unirradiation, 40, 80, and 120 kGy, respectively, clearly indicating that the change in molecular structure of the polymer matrix leads to increase in amorphousity at higher dosage.[12] The remaining residues due to degradation with increasing dose in two temperature ranges 295−330 and 540−565 °C are presented in Figure 5d, corresponding to the decomposition of host polymer chain with increased dose. The initial decomposition temperature of the thermogram for the irradiated films reveals a gradual decrease in melting temperatures (T_m) and a shift toward the lower end with dose, confirming the change in molecular structure as well as decreased weight of polymer electrolyte is a result of the creation of free radical via oxidative degradation process leading to increase in the amorphousity and decrease in crystalline region at high EB dosage.[12,29] Hence, these results confirm the influence of irradiation and are well agreed with the obtained XRD results.

3.5. Differential Scanning Calorimetry (DSC) Analysis. The change in melting temperature (T_m) and percentage of crystallinity (χ_c) of PHL10 polymer electrolytes before and after EB irradiation was investigated by differential scanning calorimetry (DSC) thermograms, as presented in Figure 6. From the DSC thermograms, the melting temperature (T_m) and melting enthalpy (ΔH_m) are determined before and after irradiation. It is observed that T_m was decreased with increase in EB dose, indicating the decrease in crystallinity. The shift in T_m of unirradiated film down from 157.39 to 153.23 °C at 120 kGy EB dose indicated the decreasing number of tie molecules in the amorphous phase by chain scission process, which simultaneously weakens the interlamellar connection upon increased irradiation dose. The significant reduction in the cohesive forces between the long-range and the intermolecular interaction between polymer chains is a reason for decrease in T_m with increase in EB dose. The decreased T_m results in decrease in crystallinity and leads to the degradation of the polymer chain at higher dosage due to chain scissoring process to destruct the crystalline region by forming defects resulting in the break in the long polymer chain at 120 kGy EB dose and hence increase in the amorphousity of the polymer electrolyte with increased EB dosage, as reported in our previous publications.[30]

The study of crystallinity (χ_c) of the irradiated polymer electrolyte is important because it is the key point influencing the conductivity of the polymer electrolyte films. The percentage of crystallinity (χ_c%) was calculated by the following equation

$$\chi\ (\%) = \frac{\Delta H_m}{\Delta H_m^\circ} \times 100 \tag{5}$$

where ΔH_m is the change in enthalpy or melting enthalpy and ΔH_m° is the heat of fusion of pure PVDF, which is equal to 104.7 J/g when the material is assumed to be 100% crystalline. The melting enthalpy (ΔH_m) was calculated by using the relation

$$\Delta H_m = \frac{\text{area under the DSC curves}}{\text{weight of the sample}} \tag{6}$$

The value of melting enthalpy (ΔH_m) and percentage of crystallinity (χ_c%) and melting temperatures of unirradiated and EB-irradiated polymer electrolyte are shown in Table 2. From the table, it clear that the values of thermal parameters for PHL10 polymer electrolyte decreased with increase in EB irradiation dose, as shown in Figure 7, and the values are lower than that of the host and unirradiated polymer electrolyte, clearly suggesting that there is a change in organic functional groups and an interruption of the polymer chains coordinate with salt systems after exposure to high radiation dose and an enhancement in the free volume regions. Therefore, the samples tend to change toward disordered state (amorphous) due to chain scission and subsequent reduction in molecular weight. The result confirms the increased amorphisity in the irradiated polymer film.[31,32] This observation is in correlation with the XRD results.

3.6. Dielectric Property of Unirradiated and Irradiated Film. The real (ε') and imaginary (ε'') parts of dielectric

DOI: 10.1021/acsomega.8b01097
ACS Omega 2018, 3, 14188−14200

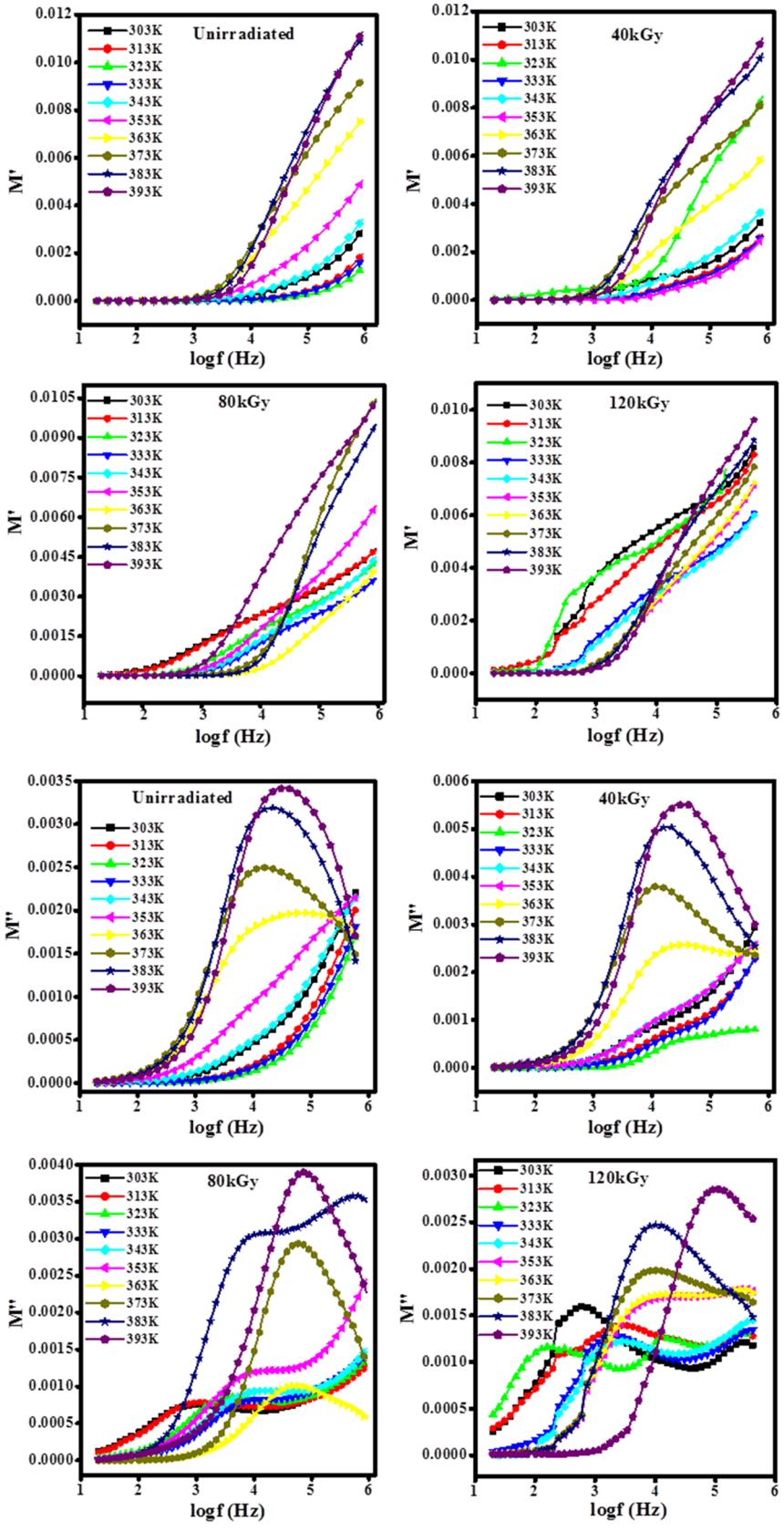

Figure 10. Variation in electric modulus as a function of frequency at different temperatures for PHL10 electrolyte films before and after irradiation.

parameters of unirradiated and irradiated PHL10 electrolyte films as a function of frequency at different temperatures are studied and presented in Figure 8. The dielectric constant (ε') of a material is related to the dipole moments polarizability,

DOI: 10.1021/acsomega.8b01097
ACS Omega 2018, 3, 14188−14200

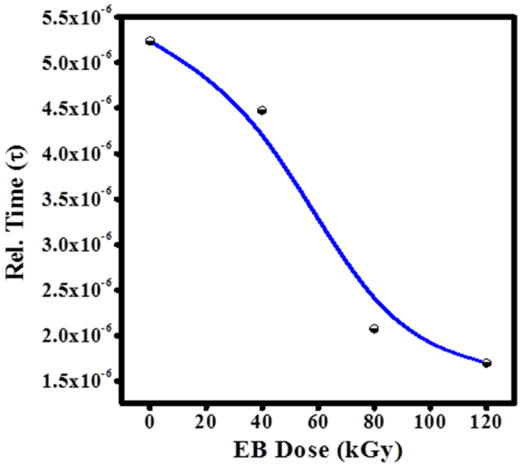

Figure 11. Variation in relaxation time (τ) as a function of the EB dose.

Table 3. Estimated DC Conductivity and Relaxation Time Values at Different EB Doses

sample name	dc cond. (S/cm)	relaxation time (τ), 10^{-6}
PHL	4.88×10^{-4}	5.239
PHL 40 kGy	3.57×10^{-4}	4.474
PHL 80 kGy	1.09×10^{-3}	2.075
PHL 120 kGy	1.81×10^{-3}	1.697

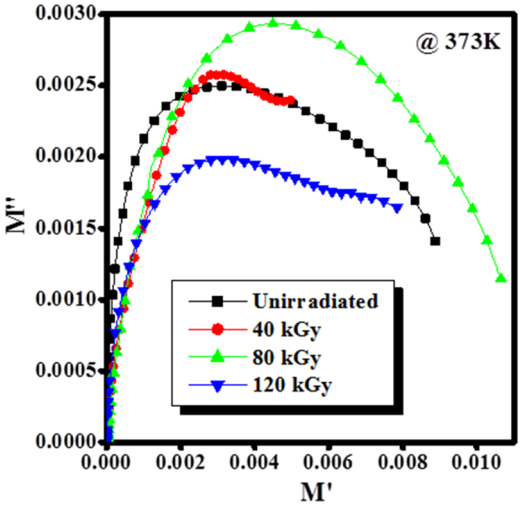

Figure 12. Cole−Cole plot of the PHL10 film before and after EB irradiation at a constant temperature of 373 K.

which arises from electric dipoles they can change the orientation of polarization subjected to the applied electric field. The dielectric behavior of polymeric materials is frequency dependent in lower frequency and frequency independent in higher frequency region.[33] The real and imaginary parts of the dielectric parameters were calculated by the following relations

$$\varepsilon' = C_p d/(\varepsilon_0 A) \tag{7}$$

$$\varepsilon'' = \varepsilon' - \tan\delta \tag{8}$$

where d is the thickness of the sample, A is the electrode area, ε_0 is the dielectric permittivity in a vacuum (8.85×10^{-12} F/m), and ω is the angular frequency.

From Figure 8, it is observed that the dielectric parameters (ε' and ε'') decrease suddenly with increase in frequency probably because dipole polarization failed to change the direction of orientation with the applied field and increase at low frequencies due to the accumulation of charges between the polymer electrolyte film and the electrode. But, it is seen that ε' and ε'' increased with temperature for unirradiated and all irradiated polymer electrolyte films because of increase in charge carrier density due to increased dissociation of ion aggregation at a higher temperature, and it obeys the universal law of dielectric response.[22]

The increasing trend of ε' at different temperatures is attributed to the formation of defects or disorders in the band gaps due to chain scissoning; it can result in more delocalization of charge carriers in electrolyte films, which confirmed the irradiation effect.[22,34]

The variation in the dielectric constant (ε') against EB at different temperatures are shown in Figure 9; it is observed that ε' increases with increased temperature. At high EB dose, the cross-linking of free radicals may stop the orientation of ions with the applied field, which leads to reduction in the population of induced free radicals, hence the polarization of trapped and bound charges failed. This process manifests that the irradiation-induced charge gradually fail to follow the applied field causing a reduction in the electronic oscillations at higher energy dosage.[35,36] It may be because of the rearrangement of amorphous phase caused by the higher energy effect of amorphous phase caused by rearrangement of atoms and redistribution of primary defects by radiation influence is region to decrease the ε' with increased EB dose.[34,37]

3.7. Electric Modulus of Unirradiated and Irradiated Film. The electric modulus $M^* = M' + iM''$, here the real (M') and imaginary (M'') parts of the complex electric modulus (M^*) correspond to energy storage and energy dissipation, respectively. The dielectric processes can be explained more clearly and accurately by modulus studies and are calculated from ε' and ε'' values using the relations

$$M' = \frac{\varepsilon'}{(\varepsilon')^2 + (\varepsilon'')^2} \tag{9}$$

$$M'' = \frac{\varepsilon''}{(\varepsilon')^2 + (\varepsilon'')^2} \tag{10}$$

The real (M') and imaginary (M'') parts of the complex modulus formalism M^* as a function of frequency for unirradiated and irradiated PHL10 electrolyte films are shown in Figure 10. It is observed that M' approaches zero at low frequency, indicating negligible contribution from electrode polarization, and increases with frequency due to lack of required amount of restoring force that governs the mobility of charge carriers under the action of an applied electric field, thereby supporting the long-range mobility corresponding to direct current (dc) conductivity. The relaxation process occurs at high frequencies, suggesting short-range mobility of charge carriers corresponding to alternating current (ac) conductivity. The relaxation curve at lower frequency indicates that facile hopping of charge carriers from one site to another causes short-range mobility, and at high frequency, the transition of charge carriers from long-range to short-range mobility leads to an increase in dc conductivity.[38]

DOI: 10.1021/acsomega.8b01097
ACS Omega 2018, 3, 14188−14200

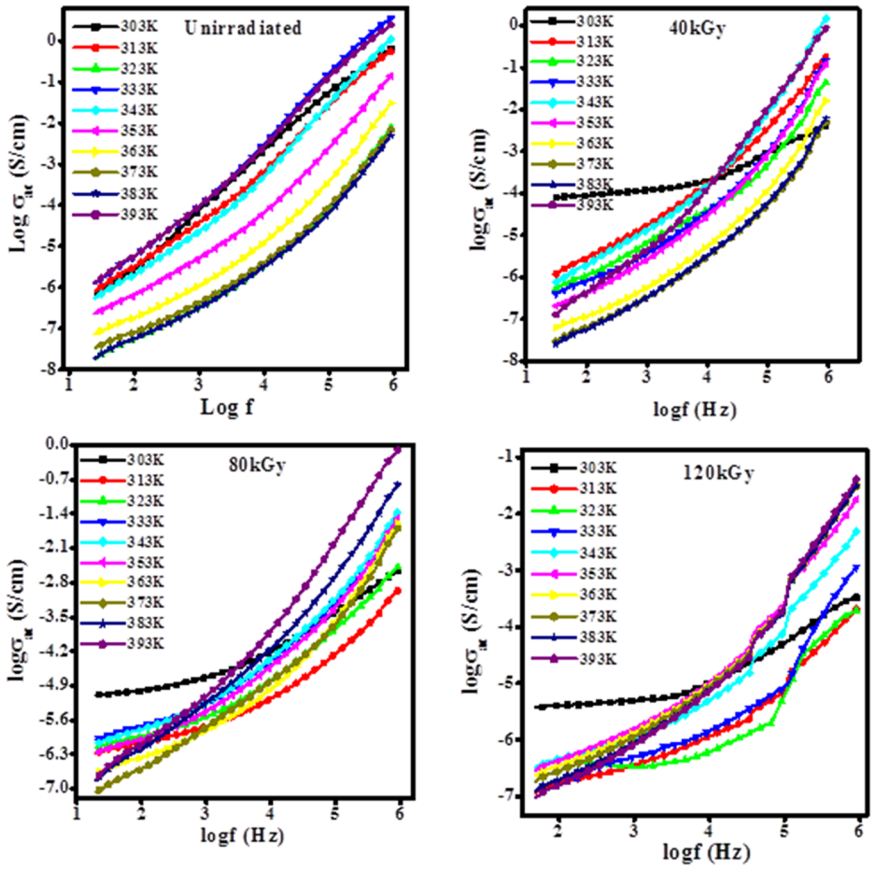

Figure 13. Variation in ac conductivity for unirradiated and irradiated PHL10 electrolyte films at different temperatures.

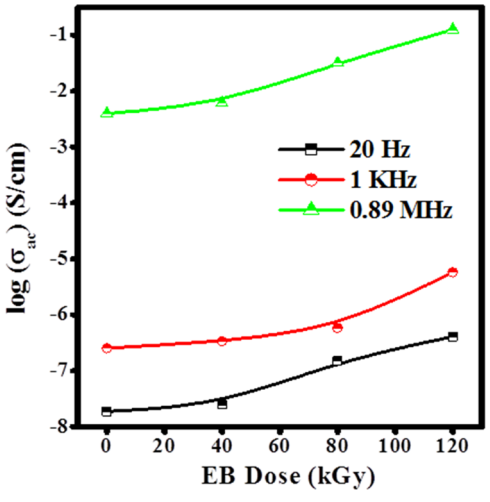

Figure 14. Variation in σ_{ac} with EB dose at different frequencies and constant temperature 383 K.

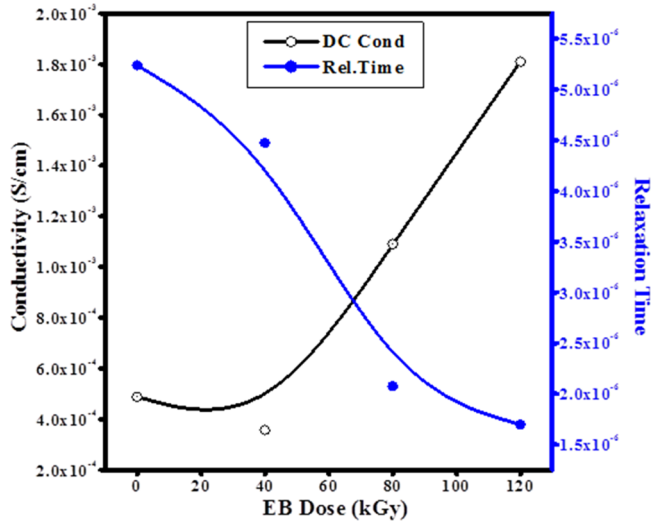

Figure 15. Variation in dc conductivity and relaxation time as a function of dose.

The shift in peak toward higher frequency with increase in temperature indicates a decrease in the relaxation time due to the distribution of free charges.[39−41] The movement of charge carriers becomes faster with increasing temperature, thus the charge carriers are thermally activated, signifying that the polymer electrolytes are ionic conductors at high temperatures. The capacitive nature of the irradiated polymer electrolyte films[39,40] was confirmed by the tail in the plots of M' versus $\log(f)$, as shown in Figure 10.

The variation in relaxation time with dose is shown in Figure 11. It is observed that the decrease in relaxation time with increasing irradiation dose assisted the formation of dipoles to follow the motion of the alternating field[39] and the lowest relaxation time (τ) 1.69×10^{-6} was observed for 120 kGy doses. The relaxation time (τ) was calculated from the maximum frequency peak position of M'' using the relation

DOI: 10.1021/acsomega.8b01097
ACS Omega 2018, 3, 14188−14200

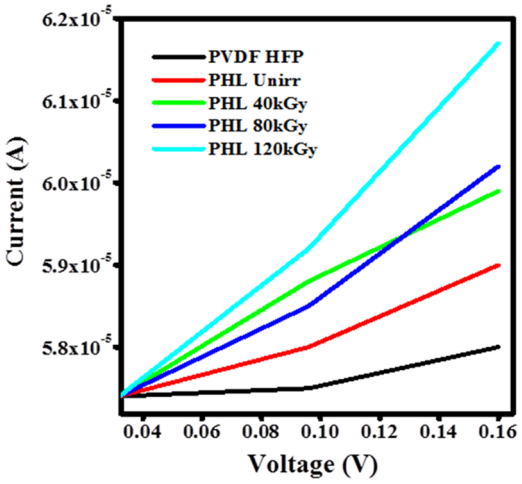

Figure 16. $I-V$ characteristics of PVDF-HFP, PHL10 unirradiated and irradiated polymer electrolyte films.

$$\tau = \frac{1}{2\pi f_{max}} \quad (11)$$

where f_{max} is the frequency, corresponding to the maximum peak position in the M'' versus $\log(f)$ plots in Figure 10, and the calculated relaxation time for unirradiated and irradiated films is presented in Table 3. The observed results confirmed that the irradiation process can change the modulus properties of the polymeric materials.

3.8. Cole–Cole Plots of Unirradiated and Irradiated Film. The Cole–Cole model was adopted to describe the dielectric relaxation process and to characterize the complex electric modulus response of materials to the electric field. The Cole–Cole plot for unirradiated and EB-irradiated PHL10 electrolyte film at different dosages and constant temperature 373 K is shown in Figure 12.

The semicircular arc observed at initial EB dose in the Cole–Cole plot is attributed to the ac conductivity contribution, it disappeared at the irradiation dose at 120 kGy is corresponds to decrease in relaxation time and attributed to segmental motions is more prominent in the amorphous region, thus it confirms the increased electrical conductivity[42,43]

3.9. AC Conductivity Study of Unirradiated and Irradiated Film. The ac conductivity of unirradiated and irradiated PHL10 polymer electrolyte films as a function of frequency is shown in Figure 13. The ac conductivity varies with frequency and temperature. The ac conductivity observed increases slightly linearly with frequency due to its disorder characteristic; there is no big change in the ac conductivity at a critical frequency (up to 5 kHz). After the critical frequency, the ac conductivity increases with frequency as it approaches the resonance frequency of the charge carriers along the polymer chain. ac conductivity is frequency independent at lower frequency due to the free charges and frequency dependent due to the release of activated trapped charges at higher frequency.[22]

The ac conductivity (σ_{ac}) was calculated by the equation

$$\sigma_{ac} = \omega c_p d \tan\delta / A \quad (12)$$

where d is the thickness of the sample, A is the electrode area, ε_0 is the dielectric permittivity in a vacuum (8.85×10^{-12} F/m), and ω is the angular frequency. The ac conductivity values for both unirradiated and irradiated films increases with irradiation dose and temperature, as shown in Figure 14, because the charge carriers are easily transported by the hopping mechanism through the defects created by radiation energy and freeing the dipoles present in the polymer chain at high temperature, in agreement with the reported results.[39,44]

Figure 14 reveals that the increase in ac conductivity with irradiation dose is attributed to the degradation of the polymer chains due to the chain scissoning resulting in reduced molecular weight at higher dosage. The low-molecular-weight polymers with salts exhibit high conductivity as compared to high-molecular-weight polymers because of reduction in the crystallinity with increased amorphous content, as reported.[10,39]

3.10. DC Electrical Conductivity of Unirradiated and Irradiated Film. The increase in dc conductivity of PHL10 polymer electrolyte film as a function of irradiation dose is shown in Figure 15. The long polymer chains break into small fragments when exposed to radiation, resulting in the modifications of the polymer matrix. As the irradiation dose increased, the polymer chain scission occurs, which provides more flexibility to ions in the polymer matrix to move easily, in turn, improving the conductivity.[12,45]

The dc conductivity of unirradiated and irradiated PHL10 polymer electrolyte films was calculated using the equation

$$\sigma_{dc} = \frac{\varepsilon_0}{M_\infty \tau} \quad (13)$$

where ε_0 is the free space permittivity, M_∞ is the frequency at which peak maximum occurs in M'', and τ is the relaxation time. It is observed that the dc conductivity of polymer electrolyte films was increased and relaxation time decreased with increase in EB dose, as shown in Figure 15. It is found that the highest conductivity of about 1.81×10^{-3} S/cm with 1.697×10^{-6} relaxation time for 120 kGy EB dose and other calculated values for different doses are given in Table 3. The decrease in crystallinity in the XRD and DSC results are well correlated with this finding.

3.11. Current–Voltage of Unirradiated and Irradiated Film. Figure 16 shows the $I-V$ characteristics of unirradiated and irradiated PHL10 polymer electrolyte films.

The current increases gradually with the applied voltage, as increasing the irradiation dose follows the Ohmic behavior; it means the current varies linearly with voltage.[38] The conductivity is due to the presence of some conjugational and trapped ions in the polymer chain as reported.[46] The increase in conductivity with increasing irradiation dose correlates well with the dielectric and electric modulus results.

3.12. NMR Spectroscopy. NMR spectrometer is used to study the polymer chain structure and dynamics and the ^{13}C NMR spectra of unirradiated and EB-irradiated PHL polymer electrolyte at 40, 80, and 120 kGy dose, as shown in Figure 17, the line narrowing observed in the ^{13}C NMR spectra with increased irradiation dose at room temperature is due to the intramolecular interactions.

The ^{13}C NMR spectra confirm the EB irradiation effect on the PHL10 polymer electrolyte by the changes reflected in the form of sharpening and splitting of the spectral lines due to the intermolecular interaction[47] with increased EB dose and exhibit new spectral lines at 162.80 ppm at 120 kGy EB dose. The NMR spectra reveals that the shift in the signal peak at 43.27 ppm in the unirradiated PHL polymer electrolyte to 43.51 ppm after 120 kGy EB dose is attributed to the presence

DOI: 10.1021/acsomega.8b01097
ACS Omega 2018, 3, 14188–14200

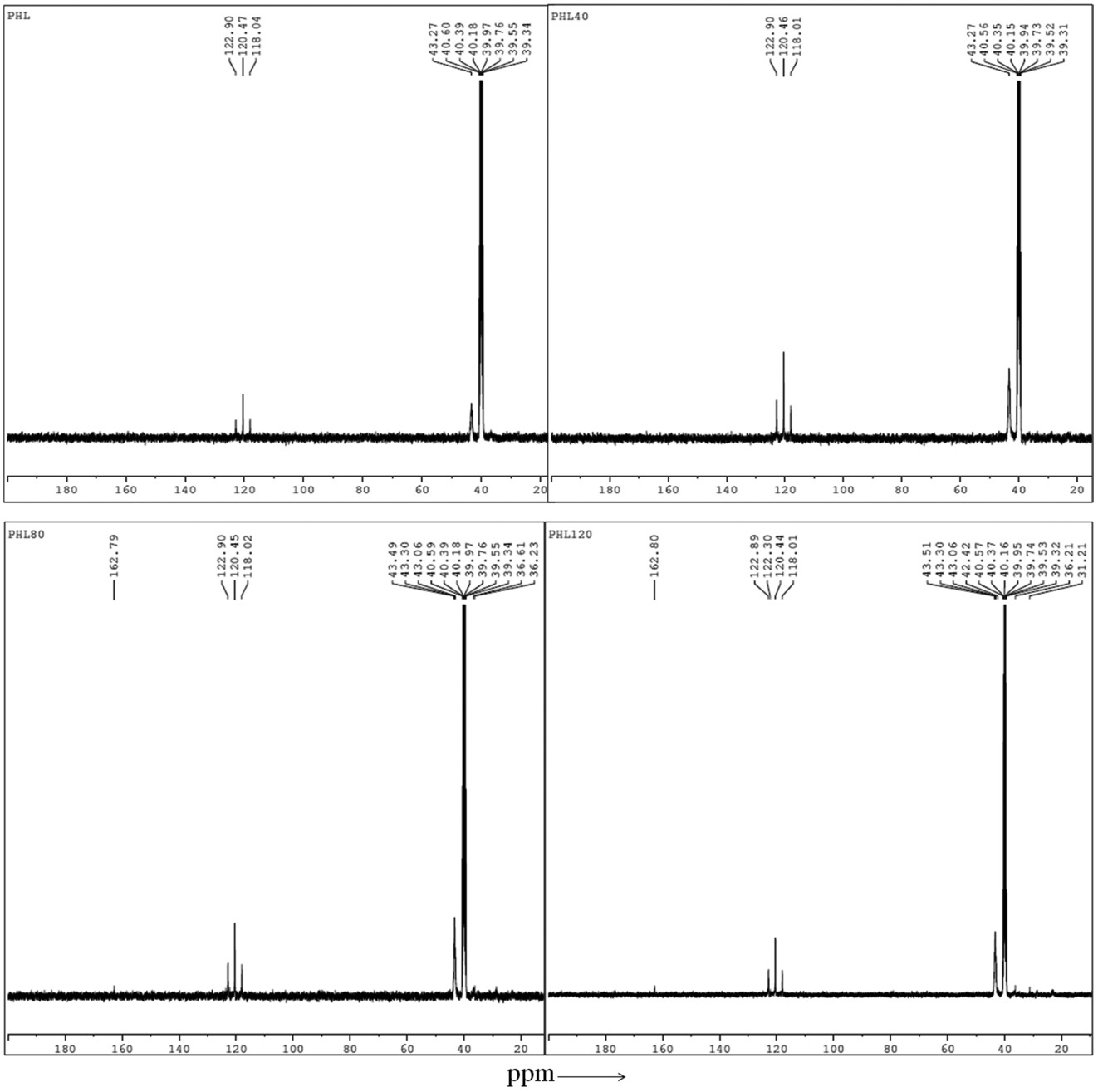

Figure 17. ^{13}C NMR spectra of unirradiated and EB-irradiated PHL10 polymer electrolyte at 40, 80, and 120 kGy doses.

of carbon atoms and fluorinated carbon atoms in the peak range 118−122 ppm, and the spectral lines between 118 and 121 ppm are assigned to the CF_2 group of the host polymer. The NMR study confirms that relative change in chemical bonds and radiation-induced changes in polymeric materials due to irradiation results in degradation of the polymer electrolyte upon irradiation,[48] and the results are in good agreement with FT-IR analysis.

3.13. Electrochemical Performance. The electrochemical performance of unirradiated and EB-irradiated PHL10 polymer electrolyte was studied by using cyclic voltammetry (CV) within −3−1 V potential window in a three-electrode system at room temperature. Pt wire is used as a counter electrode, Ag/AgCl as a reference electrode, and glassy carbon as a working electrode placed in the polymer electrolyte solution prepared in dimethylformamide (DMF) solvent. The *C*−*V* curves of PHL10 polymer electrolyte before and after irradiation is presented in Figure 18a and that of EB-irradiated PHL10 at 120 kGy with 30, 60, and 90 mV/s scan rates are given in Figure 18b.

The unirradiated electrolyte reveals an ideal shape with a less integrated area under CV curves without a redox peak. After EB irradiation to radiation, the area under the *C*−*V* curves increases significantly with a clear redox peak at around −0.9 V and is increased with increase EB dose as shown in Figure 18a, it represents the charge and discharge processes occur reversibly at the electrolyte interface; is confirms the capacitive nature of irradiated polymer electrolytes. Figure 18b represents the *C*−*V* curves of 120 kGy EB dose irradiated PHL10 polymer electrolyte at 30, 60, and 90 mV/s scan rates. It reveals the increased redox reaction process with increased scan rate, the oxidation and reduction peak currents increase

DOI: 10.1021/acsomega.8b01097
ACS Omega 2018, 3, 14188−14200

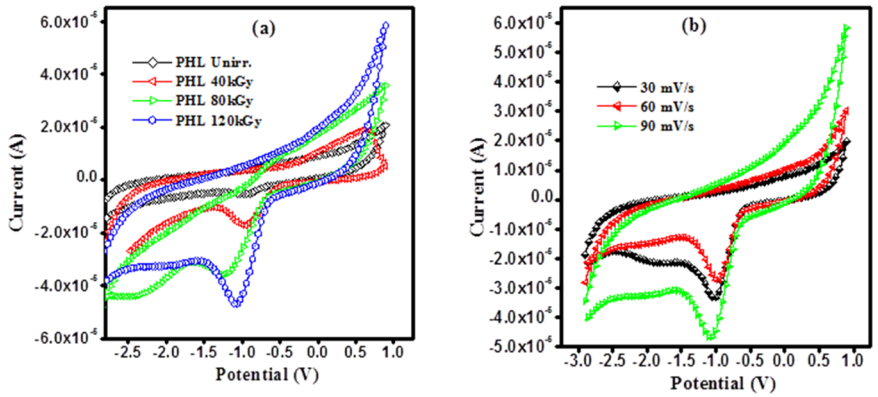

Figure 18. Cyclic voltammetry curves of PHL10 polymer electrolyte film: (a) unirradiated, 40, 80, and 120 kGy EB dose and (b) 120 kGy EB dose at different scan rates.

significantly.[48−50] The results reveal that the polymer electrolytes are electrochemically active after EB irradiation and are active materials for potential storage and lithium-ion battery applications.

4. CONCLUSIONS

The PHL10 polymer electrolyte films were prepared by solution-casting method and the effect of EB irradiation effect at 40, 80, and 120 kGy doses was studied. The change in the surface roughness was observed after EB irradiation in PHL10 electrolyte film confirms the morphological change due to the irradiation effect. FT-IR results confirmed the effect of EB dose on the structural properties of the polymer electrolytes by change in the peak intensity and shifting peak positions after irradiation. The NMR study confirms the degradation and radiation-induced changes in polymeric materials. The XRD analysis confirms the increased amorphous phase by decreasing crystallinity upon the increased EB dose and the decrease in the melting temperature of polymer electrolyte confirms that the degradation of the polymer chain is resulted by chain scission process upon irradiation. Thermal properties varied with increased irradiation dose and the percentage of crystallinity decreased from 49.87 for unirradiation to 33.05 after irradiation with 120 kGy EB; the finding was confirmed by the DSC analysis. The changes in dielectric parameters with increased EB irradiation dose confirms the formation of cross-linked free radicals with applied high EB dose. These results confirm that the physiochemical properties of the polymer electrolytes can be changed by EB irradiation for possible commercial applications. The increase in conductivity with increased EB dose is attributed to the degradation of the polymer chains due to the chain scission results in the reduced molecular weight at a higher dosage and the PHL10 polymer electrolyte exhibits an electrical conductivity 1.8×10^{-3} S/cm after irradiated with 120 kGy EB dose. The $C-V$ curves reveal that the PHL10 polymer electrolyte is electrochemically active and exhibits capacitive behavior by redox reaction at different scan rates upon irradiation. The observed results confirm the change in physical properties of polymer electrolytes by EB irradiation at different doses, and that irradiated polymeric materials may have potential application in commercial applications as well as optoelectronic devices and battery applications.

Scheme 1. Synthesis Process of Polymer Electrolyte Preparation and Chain Scissoring Phenomenon Due to Irradiation

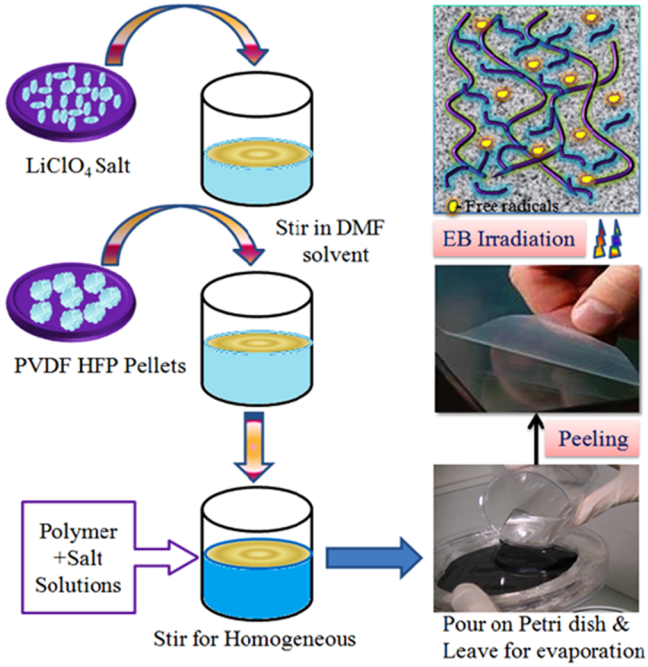

5. EXPERIMENTAL METHODS

5.1. Materials. Poly((vinylidene fluoride)-*co*-hexafluoropropylene) pellets (PVDF-HFP; M_w: 455 000 g/mol) and lithium perchlorate ($LiClO_4$-M_w: 106.4 g/mol) were purchased from Sigma-Aldrich. Dimethylformamide (DMF, M_w: 73.09 g/mol) was from Merck, India.

5.2. Preparation of PHL10 Electrolyte Film. The polymer electrolyte film was prepared by solution-casting method. The PVDF-HFP/$LiClO_4$ (90:10 w/w, coded as PHL10) weight ratios were dissolved separately in dimethylformamide (DMF−C_3H_7NO) solvent by stirring continuously for about 6−8 h at room temperature. The solutions were then mixed by stirring continuously till a homogeneous viscous solution was obtained. Then, the solution was cast onto a Petri dish and allowed to evaporate and peel off the bulk free stand film. The thickness of the free standing film, around 0.30−0.35 mm, was measured using a screw gauge. The mechanism of the solution-casting process is shown in Scheme 1.

DOI: 10.1021/acsomega.8b01097
ACS Omega 2018, 3, 14188−14200

5.3. Polymer Electrolyte Films Exposed to 8 MeV Electron Beam Energy. 8 MeV electron beam (EB) energy was used to irradiate the PHL10 electrolyte films with 260 mA current at 31 Hz pulse repetition rate as well as pulse width of 10 μS and conveyor speed of 1.3 m/min scanning −4.0 A@ 200 ms at 40, 80, and 120 kGy dosage in LINAC, Raja Ramanna Centre for Advanced Technology, Indore, India.

AUTHOR INFORMATION

Corresponding Author

*E-mail: dehu2010@gmail.com.

ORCID

Vijeth Hebri: 0000-0002-3352-9002

Devendrappa Hundekal: 0000-0002-7565-862X

Notes

The authors declare no competing financial interest.

ACKNOWLEDGMENTS

Author would like to thank DAE-BRNS for sanctioning the major research project (letter No. 34(1)/14/39/2014-BRNS/ dated 10-12-2014) and PURSE Mangalore University Mangalore for TGA facility and Bangalore University Bangalore for providing XRD facility.

REFERENCES

(1) Kumar, H. G. H.; Mathad, R. D.; Ganesh, S.; Sarma, K. S. S.; Haramaghatti, C. R. *Braz. J. Phys.* **2011**, *41*, 7−14.

(2) Chmielewski, A. G.; Haji-Saeid, M.; Ahmed, S. *Nucl. Instrum. Methods Phys. Res., Sect. B* **2005**, *236*, 44.

(3) Singh, L.; Samra, K. S.; Singh, R. *Nucl. Instrum. Methods Phys. Res., Sect. B* **2007**, *255*, 350.

(4) Fares, S. *Am. J. Mater. Sci.* **2011**, *1*, 52−56.

(5) Sinha, D.; Sahoo, K. L.; Sinha, U. B.; Swu, T.; Chemseddine, A.; Fink, D. *Radiat. Eff. Defects Solids* **2004**, *159*, 587−595.

(6) Ma, Y.-Z.; Li-Long, P.; Ya-Bin, Z.; Zhi-Guang, W.; Tie-Long, S. *Chin. Phys. B* **2011**, *20*, No. 078104.

(7) Gaafar, M. S.; El-Wakil, A. A.; Mirham, A. B. *Arch. Appl. Sci. Res.* **2013**, *5*, 158−166.

(8) Abdul-Kader, A. M. *Philos. Mag. Lett.* **1989**, *3*, 162−169.

(9) Othon, C. M.; Ducharme, S. *Ferroelectrics* **2004**, *304*, 9−12.

(10) Saikia, D.; Kumar, A.; Singh, F.; Avasthi, D. K.; Mishra, N. C. *J. Appl. Phys.* **2005**, *98*, No. 043514.

(11) Tang, Y.; Xing-Zhong, Z.; Chan, H. L. W.; Choy, C. L. *Appl. Phys. Lett.* **2000**, *77*, 1713.

(12) Raghu, S.; Archana, K.; Sharanappa, C.; Ganesh, S.; Devendrappa, H. *J. Non-Cryst. Solids* **2015**, *426*, 55−62.

(13) Xie, H.; Zhiyuan, T.; Zhongyan, L.; Yanbing, H.; Yong, L.; Hong, W. *J. Solid State Electrochem.* **2008**, *12*, 1497.

(14) Ramesh, S.; Ong, P. L. *Polym. Chem.* **2010**, *1*, 702.

(15) Ataollahi, N.; Ahmad, A.; Hamzah, H.; Rahman, M. Y. A.; Mohamed, N. S. *Int. J. Electrochem. Sci.* **2012**, *7*, 6693−6703.

(16) Khayet, M. *Appl. Surf. Sci.* **2004**, *238*, 269−272.

(17) Nathawat, R.; Kumar, A.; Vijay, Y. K. In Morphological Changes of Electron-Beam Irradiated PMMA Surface, Proceedings of PAC07; IEEE: Albuquerque, NM, 2007; p 4244.

(18) Jayanthi, S.; Sundaresan, B. *Ionics* **2015**, *21*, 705−717.

(19) Prabakaran, K.; Smita, M.; Nayak, S. K. *RSC Adv.* **2015**, 40491−40504.

(20) Ulaganathan, M.; Nithya, R.; Rajendran, S.; Raghu, S. *Solid State Ionics* **2012**, *218*, 7−12.

(21) Cataldi, P.; Bayer, I. S.; Cingolani, R.; Marras, S.; Chellali, R.; Athanassiou, A. *Sci. Rep.* **2016**, *6*, No. 27984.

(22) Raghu, S.; Subramanya, K.; Ganesh, S.; Nagaraja, G. K.; Devendrappa, H. *Radiat. Phys. Chem.* **2014**, *98*, 124−131.

(23) Nasef, M. M.; Saidi, H.; Dahlan, K. Z. M. *Radiat. Phys. Chem.* **2003**, *68*, 875−883.

(24) Ataollahi, N.; Ahmad, A.; Hamzah, H.; Rahman, M. Y. A.; Mohamed, N. S. *Int. J. Electrochem. Sci.* **2012**, *7*, 6693−6703.

(25) Yesappa, L.; Niranjana, M.; Ashokkumar, S. P.; Vijeth, H.; Basappa, M.; Jishnu, D.; Petwal, V. C.; Ganesh, S.; Devendrappa, H. *RSC Adv.* **2018**, *8*, 15297.

(26) Jaleh, B.; Negin, G.; Parisa, F.; Nakatan, M.; Soheil, M. T. *Membranes* **2015**, *5*, 1−10.

(27) Neelakandan, S.; Rana, D.; Matsuura, T.; Muthumeenal, A.; Kanagaraj, P.; Nagendran, A. *Solid State Ionics* **2014**, *268*, 35−41.

(28) El All, S. A. *J. Phys. D: Appl. Phys.* **2007**, *40*, 6014−6019.

(29) Medeiros, A. S.; Gual, M. R.; Pereira, C.; Faria, L. O. *Radiat. Phys. Chem.* **2015**, *116*, 345−348.

(30) Yesappa, L.; Niranjana, M.; Ashokkumar, S. P.; Vijeth, H.; Ganesh, S.; Devendrappa, H. *Radiat. Eff. Defects Solids* **2018**, 601−607.

(31) Zhang, K.; Cui, Z.; Xing, G.; Feng, Y.; Meng, S. *RSC Adv.* **2016**, No. 100079.

(32) Atanassov, A.; George, K.; Dimitrina, K.; Ljudmila, B. K. J. *J. Thermoplast. Compos. Mater.* **2012**, 1−16.

(33) Singh, N. L.; Shah, S.; Qureshi, A.; Tripathi, A.; Singh, F.; Avashti, D. K.; Raole, P. M. *Bull. Mater. Sci.* **2011**, *34*, 81−88.

(34) Peng, G.; Zhao, X.; Zhan, Z.; Shengzong, C.; Wang, Q.; Liang, Y.; Zhao, M. *RSC Adv.* **2014**, *4*, 16849.

(35) Rana, D. S.; Chaturvedi, D. K.; Quamara, J. K. *Optoelectron. Adv. Mater., Rapid Commun.* **2009**, *3*, 1354−1358.

(36) Singh, N. L.; Shah, S.; Qureshi, A.; Tripathi, A.; Singh, F.; Avasthi, D. K.; Raole, P. M. *Bull. Mater. Sci.* **2011**, *34*, 81−88.

(37) Kulkarni, S.; Nagabhushana, B. M.; Parvatikar, N.; Shivakumara, C.; Damle, R. *ISRN Mater. Sci.* **2011**, No. 808560.

(38) Najar, M. H.; Majid, K.; Abdullah Dar, M. *J. Mater. Sci.: Mater. Electron.* **2017**, *17*, 6913−6917.

(39) Raghu, S.; Kilarkaje, S.; Sanjeev, G.; Devendrappa, H. *Radiat. Meas.* **2013**, *53*−*54*, 56−64.

(40) Das, S.; Ghosh, A. *J. Phys. Chem. B* **2017**, *121*, 5422−5432.

(41) Tsangaris, G. M.; Psarras, G. C.; Kouloumbi, N. *J. Mater. Sci.* **1998**, *33*, 2027−2037.

(42) Jiang, X.; Zhao, X.; Peng, G.; Liu, W.; Liu, K.; Zhan, Z. *Curr. Appl. Phys.* **2017**, *17*, 15−23.

(43) Tsangaris, G. M.; Psarras, G. C.; Kouloumbi, N. *J. Mater. Sci.* **1998**, *33*, 2027−2037.

(44) Abdel-Hamid, H. M. *Solid-State Electron.* **2005**, *49*, 1163−1167.

(45) Kim, M.; Jun-Young, S.; Chang Nho, Y.; Tae-Woo, L.; Jong Hyeok, P. *J. Electrochem. Soc.* **2010**, *157*, A31−A34.

(46) Naqash, W.; Majid, K. *Mater. Res.* **2015**, *18*, 1121−1127.

(47) Lalia, B. S.; Yamada, K.; Hundal, M. S.; Jin-Soo, P.; Gu-Gon, P.; Won-Yong, L.; Chang-Soo, K.; Sekhon, S. S. *Appl. Phys. A* **2009**, *96*, 661−670.

(48) Yesappa, L.; Niranjana, M.; Ashokkumar, S. P.; Vijeth, H.; Basappa, M.; Jishnu, D.; Petwal, V. C.; Ganesh, S.; Devendrappa, H. *RSC Adv.* **2018**, *8*, 15297−15309.

(49) Fattah, N. F. A.; Ng, H. M.; Mahipal, Y. K.; Arshid, N.; Ramesh, S.; Ramesh, K. *Materials* **2016**, *9*, No. 450.

(50) Karuppasamy, K.; Hyun-Seok, K.; Dongkyu, K.; Vikraman, D.; Prasanna, K.; Kathalingam, A.; Sharma, R.; Rhee, H. W. *Sci. Rep.* **2017**, *7*, No. 11103.

DOI: 10.1021/acsomega.8b01097
ACS Omega 2018, 3, 14188−14200